PNAS RESEARCH ARTICLE | MEDICAL SCIENCES

A step toward precision gerontology: Lifespan effects of calorie and protein restriction are consistent with predicted impacts on entropy generation

Ayşe Selcen Semercioöz-Oduncuoğlu[a,b,1], Sharon E. Mitchell[b,1], Mustafa Özilgen[a], Bayram Yilmaz[c,2], and John R. Speakman[b,d,e,2]

Contributed by John R. Speakman; received January 20, 2023; accepted July 12, 2023; reviewed by James E. Cleaver and Joao Pedro Magalhaes

Understanding aging is a key biological goal. Precision gerontology aims to predict how long individuals will live under different treatment scenarios. Calorie and protein restriction (CR and PR) extend lifespan in many species. Using data from C57BL/6 male mice under graded CR or PR, we introduce a computational thermodynamic model for entropy generation, which predicted the impact of the manipulations on lifespan. Daily entropy generation decreased significantly with increasing CR level, but not PR. Our predictions indicated the lifespan of CR mice should increase by 13 to 56% with 10 to 40% CR, relative to ad libitum-fed animals. This prediction was broadly consistent with the empirical observation of the lifespan impacts of CR in rodents. Modeling entropy fluxes may be a future strategy to identify antiaging interventions.

entropy | aging | calorie restriction | protein restriction

Significance

The lifespan entropy concept suggests that entropy increases in living organisms through time. Death happens when entropy becomes incompatible with life. We introduced a bio-thermodynamic approach to quantify rates of entropy generation and used it to predict the lifespan expected for mice exposed to variable levels of calorie and protein restriction (CR and PR). We found that entropy generation was reduced under CR and correlated with the CR level. This allowed a rough prediction of longevity at the group level. The improved and extended application of this kind of thermodynamic approach might be a stepping stone toward predicting individual lifespans and a promising tool to evaluate longevity therapeutics.

Almost all organisms age and die, but they do so at different rates, both within and among species. Predicting the aging and lifespan consequences of different lifestyles and physiologies, also called precision gerontology, is a key scientific goal. While predicting individual lifespan may be complex and subject to stochastic events, a stepping stone toward precision gerontology is to be able to predict the outcome of manipulations at the population level. That is if a population A is subjected to some manipulation or drug, we may not be able to predict if individual 1 within this population will live longer than individual 2 in the same population, but we may be able to predict on average if the individuals in population A will live longer than those in population B that has not been exposed to the manipulation. Developing a unifying framework that may be able to predict the gerontological consequences of diverse manipulations is therefore a major step forward in precision gerontology, and would be a major aid in the development and screening of antiaging interventions.

In his book "What is life?" Erwin Schrodinger (1944) presented a hypothesis for why organisms age and die (1). His main hypothesis was that living animals are in a state of low entropy. This entropy increases over the lifespan until it reaches a point where the system can no longer function effectively and the organism dies. This also implies that aging is the manifestation of entropy increasing in the system. The basis of this physical model is that life generates entropy, which accumulates in the organism because it cannot be, or becomes too expensive, to eliminate. Entropy is the quantitative expression of the molecular irregularity or disorder within the system boundaries (2). Entropy can be transferred through the system boundaries via mass and heat. The following entropy balance Eq. **1** can be used for any system to calculate entropy generation by the system (2):

$$\sum_{\text{in}}(\dot{m}s)_{\text{in}} - \sum_{\text{out}}(\dot{m}s)_{\text{out}} - \sum \frac{\dot{q}}{T_{b,i}} + \dot{s}_{\text{gen}} = \frac{d(ms)_{\text{system}}}{dt} \qquad [1]$$

where, the first two terms in the equation refer to the entropy, s, input and output, respectively, via mass flux, $\dot{m}$, through the system boundaries. The third term is the entropy that accompanies to the heat flux, $\dot{q}$, across the system boundaries. The last term at the left side is entropy generation, $\dot{s}_{\text{gen}}$, by the system as a result of irreversibilities. Çengel et al. (2) especially emphasized in his pioneering thermodynamics book that this term refers the entropy generation within the system boundary only (2). The term at the right side refers to the entropy change of the system. In this framework, a living organism is selected as subsystem boundaries to be analyzed (Fig. 1) within a wider open system (i.e., control volume). To be able to conduct the analyses for the living state, we are assuming there is a steady-flow across the organism subsystem boundaries and the right side of the

Author contributions: A.S.S.-O., S.E.M., B.Y., and J.R.S. designed research; A.S.S.-O., S.E.M., M.Ö., B.Y., and J.R.S. performed research; A.S.S.-O., S.E.M., M.Ö., B.Y., and J.R.S. analyzed data; and A.S.S.-O., S.E.M., M.Ö., B.Y., and J.R.S. wrote the paper.

Reviewers: J.E.C., University of California, San Francisco; and J.P.M., University of Birmingham.

The authors declare no competing interest.

[1]A.S.S.-O. and S.E.M. contributed equally to this work.

[2]To whom correspondence may be addressed. Email: byilmaz@yeditepe.edu.tr or j.speakman@abdn.ac.uk.

This article contains supporting information online at https://www.pnas.org/lookup/suppl/doi:10.1073/pnas.2300624120/-/DCSupplemental.

Published September 5, 2023.

equation is considered zero (2). Therefore, for a steady-flow open system, the entropy generation within the system boundaries can be calculated by considering mass and heat flows across the system boundaries. In brief, the entropy generation constituent of the selected steady-flow open system is the lost useful energy, other than the entropy transferred with mass (e.g., food, O_2, CO_2, H_2O, feces etc.) and heat (e.g., heat flux due to temperature difference between the system and environment), as introduced at Eq. **1**.

Cumulative entropy generation within the living system boundaries throughout life is referred to as the "lifespan entropy," and the "entropic age" concept suggests that aging-related changes are linked to entropy generation (S_{gen}) (3, 4). During homeostasis, organisms import energy and generate entropy (5). The continuous and inevitable entropy generation in the system ultimately leads to death when animals reach thermodynamic equilibrium with their surroundings (6). By this model, all living beings die after generating a certain amount of lifespan entropy, since their bodies cannot tolerate becoming more disordered. The concept of lifespan entropy generation therefore provides a framework for developing precision gerontological predictions at the population, and ultimately potentially at the individual, level. Lifespan entropy generation has been suggested to depend on various factors such as body size (7), heat transfer from the body to the environment (hence body temperature) (8, 9), physical activity (6) and the composition of the diet (10, 11). Despite this strong theoretical background, the entropy hypothesis has not yet been empirically tested.

Calorie restriction (CR) is one of the few experimental manipulations that has been repeatedly shown to extend lifespan and improve health span by retarding the rate of aging across a range of organisms (12–14). The effect of CR on lifespan depends on the level of restriction, with a linear, but highly variable effect in mice and other rodents up to at least 65% restriction (15). There has been some debate over whether the impact of CR is a consequence of reduced energy intake, or the simultaneous restriction of protein (PR) (16, 17). A review of the impacts of energy and protein concluded that CR and PR have independent effects in rodents, but the impact of CR on lifespan is about 10× greater (18). The impacts of CR and PR on lifespan provide an ideal model to test the entropy generation theory of aging. In the present study, we estimated the daily average entropy generated by the cellular metabolism of mice undertaking 3-mo long CR and PR interventions. Six subsystems were employed in the model to perform the thermodynamic analyses of different CR and PR levels within the context of first and second laws (Fig. 1). These were cellular metabolism, adipose tissue, invested organs (i.e., organs that grow under restriction), utilized organs (i.e., organs that shrink under restriction), muscular tissue and the internal work sink. Thermodynamic data were used to estimate the lifespan implications of CR and PR under the lifespan entropy generation theory. Finally, these predictions were compared to empirical lifespan data for manipulations of rodents. The evaluated results showed us second law of thermodynamics assessments might be a promising and useful tool to predict the approximate lifespan of mice exposed to different levels of CR.

Results

First Law Assessment of Cellular Metabolism Subsystem. Especially in the biothermodynamics field, the internal energy content of a chemical compound is called enthalpy (19). The standard enthalpy of formation (Δh°_f) values of the major chemical components in the diets and their oxidation reaction products (*SI Appendix*, Table S1) were used to calculate the daily enthalpy of oxidation reaction (Δh_{rxn}) of the diets for CR and PR groups. In this study, Δh_{rxn} refers to the extracted energy (kJ) at the cellular level (*SI Appendix*, Fig. S1). Δh_{rxn} levels were higher in mice fed PR compared to CR due to the reduced protein levels being replaced by carbohydrate while maintaining the same total calorie intake across the PR groups (*SI Appendix*, Fig. S1). This causes very similar work outputs (kJ) fueled by cellular metabolism of the PR groups (19.5 to 20.2 kJ). In the CR groups, average daily total work (kJ) output fueled by the cellular metabolism decreased with the increasing CR level (R-square > 0.99, $P < 0.05$). The CR animals might compensate for low-energy input with decreased total work performance (*SI Appendix*, Fig. S2 *A* and *B*). There was no significant relationship between average daily total work (kJ) output fueled by the cellular metabolism and level of PR. The ratio of this work to the net extracted energy by the cellular metabolism subsystem was defined as the first law efficiency. There was no significant relationship between the average daily first law

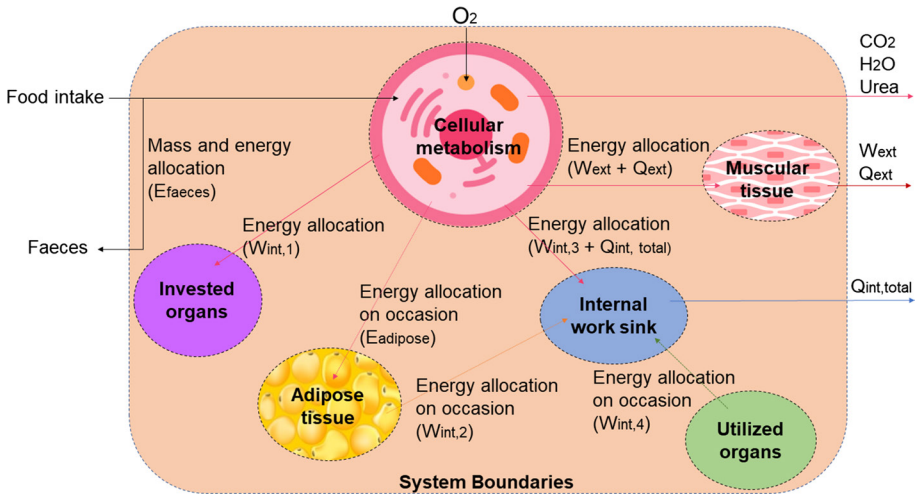

Fig. 1. The thermodynamic system and subsystems boundaries. $W_{int,1}$ and $W_{int,3}$ refer to the energy allocation from cellular metabolism to organ investment and internal works, respectively; $W_{int,2}$ refers to energy allocation from adipose tissue to internal works; $W_{int,4}$ refers to energy allocation from utilized organs to internal works; W_{ext} refers to muscular work; Q_{ext} and Q_{int} refer to the produced heat due to muscular and internal works, respectively; E_{feces} and $E_{adipose}$ refer to energy allocation to feces and adipose tissue, respectively.

efficiency (%) and energy intakes (kJ) or restriction levels (%) of CR and PR groups (*SI Appendix*, Fig. S4 *A* and *C*).

Second Law Assessments of Cellular Metabolism Subsystem. Within the context of the second law of thermodynamics, the exergy term basically refers to the "maximum useful work potential" that a system can produce if it is brought to thermodynamic equilibrium with its surroundings. Hence, it is a system–environment combination property. Unlike energy, exergy is always wasted in irreversible processes and this wasted work potential is defined as exergy destruction (Ex_{dest}) (2). In the current study, the exergy values (kJ) of chemical molecules of diet, adipose tissue and oxidation reactions' products were calculated based on the mole numbers of molecules and the daily average body temperature of CR and PR animals. All these calculated values were used in exergy balance (Eq. **17**), which was equated around the cellular metabolism subsystem (Fig. 1) to find the daily Ex_{dest} of the animals. One of the ultimate aims of this study was the calculation of daily entropy generation, S_{gen}, (kJ/K) via cellular metabolism. Hence, daily average body temperature and calculated daily Ex_{dest} values were used for this purpose via Eq. **19** as explained in the *Materials and Methods*.

The second law efficiency was defined in this study as the ratio of work flux fueled by cellular metabolism to the maximum theoretical exergy (Eq. **18**). The average daily second law efficiency of CR groups (*SI Appendix*, Fig. S4*B*) was significantly related to the exergy input of CR groups (R-square > 0.78, $P < 0.05$). However, no relationship was found with the PR groups (*SI Appendix*, Fig. S4*D*). In the present study, internal work components ($W_{int,1} + W_{int,3}$) had a dominant effect on the total work expense that was fueled by the cellular metabolism subsystem and these work components had a decreasing contribution with increasing CR level (*SI Appendix*, Fig. S5*A*). In contrast, the exergy input and corresponding internal work components fueled by cellular metabolism across the PR levels and 24 h ad libitum (24AL) were very similar (*SI Appendix*, Fig. S5*B*). The effect of external (muscle) work (W_{ext}) on second law efficiency was very low under both CR and PR conditions (*SI Appendix*, Fig. S4 *A* and *B*). A major increase (more than four times) in average daily external (muscle) work was observed in both CR and PR groups exposed to restriction levels higher than 9.6% probably because of increased hunger (20, 21) which has been linked to the resultant food anticipatory activity (22) (*SI Appendix*, Fig. S5 *A* and *B*).

The calculated daily entropy generation (kJ/K) values by using the daily exergy destruction values are given in *SI Appendix*, Fig. S6 *A* and *B*. The average daily entropy generation was found to decrease with increasing CR level (%) (Fig. 2*A* and *SI Appendix*, Fig. S6*A*) or in other words decreasing exergy intake (R-square > 0.99, $P < 0.05$). Similarly in another thermodynamic assessment study (11), the entropy generated by the cellular metabolism subsystem increased with increments in the average exergy intake (R-square > 0.99, $P < 0.05$) in obese and lean rats. On the other hand, for the PR groups, there was no significant relationship between the average daily entropy generation and PR levels (%) ($P > 0.05$) (Fig. 2*B* and *SI Appendix*, Fig. S6*B*) but if we consider the exergy intake (kJ) of PR groups instead of restriction levels (Fig. 2*C*), a significant relationship with entropy generation rates is clear (R-square > 0.93, $P < 0.05$).

The average daily entropy generation (kJ/K) by the CR groups was positively related to the work output fueled by the cellular metabolism (kJ) (R-square > 0.97, $P < 0.05$) (Fig. 2*A* and *SI Appendix*, Fig. S2). A similar linear relationship between work output and entropy generation was computationally estimated using experimental energetic datasets (23–26). Both internal (i.e., respiration, cardiac

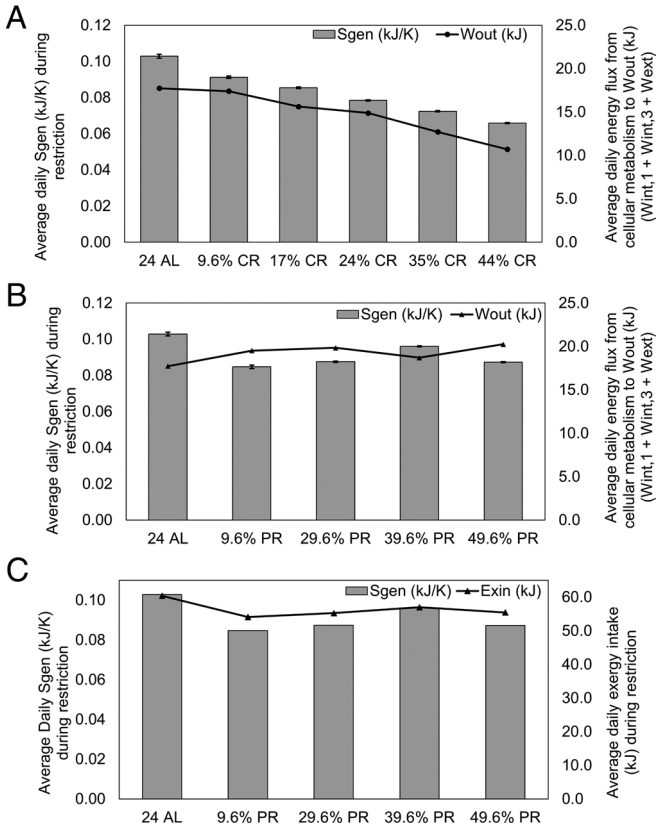

Fig. 2. Average daily entropy generation (S_{gen}) and fueled work output (W_{out}) by cellular metabolism in male C57BL/6 mice under 3 mo of (*A*) CR or (*B*) PR and (*C*) relationship between S_{gen} and average daily exergy intake (Ex_{in}) of PR groups. The level of restriction shown refers to measured energy intakes in the final week of study relative to 24AL fed mice. Error bars are ±SEM of each group's daily values over the 80 d.

functions, signal transmission through the neurons etc.) and external or muscular (i.e., energy consumption for the skeletal muscle contraction to move external objects or the animals' own body) work are irreversible processes in a living system that, as the second law of thermodynamics states, result in entropy generation. No relationship between average daily total work output and entropy generation was observed under PR ($P > 0.05$).

The entropy generation hypothesis suggests that animals die when their entropy generation (or in other words, molecular disorder) levels reach a certain level (1). The problem is that the level at death is unknown. However, we do know the average lifespan of unrestricted C57BL/6 mice and hence we can combine that with the calculated average daily entropy generation rates derived here to estimate the lifespan entropy in that situation, and then quantitatively predict the impacts of altered entropy generation rates (Fig. 2*A*) on the expected lifespans of CR and PR mice. Table 1 shows that, with 9.6 to 44% restriction in calorie intake, the predicted lifespan increases by 91 to 405 d compared to the 24AL group. PR mice have a higher energy or exergy intake, and higher entropy generation rates than those of mice fed an equivalent CR level (Fig. 2 *A* and *B*). As a result, the predicted lifespan increments of the PR groups (51 to 154 d) were lower compared to the CR groups.

Discussion

First and Second Law Efficiencies. From the first law efficiency calculations, approximately 37% of the net daily food energy extracted by the cellular metabolism was used to fuel internal and muscle work for the 24AL group. Note the first law efficiency

Table 1. Calculated lifespan predictions of CR and PR animals

Groups	Predicted lifespan (day)* based on entropy generation	Predicted lifespan (day)* based on regression equations extracted from reviewed empirical lifespan data (18)
44% CR	1,125	952
35% CR	1,022	904
24% CR	945	846
17% CR	867	809
9.6% CR	811	771
49.6% PR	848	790
39.6% PR	771	780
29.6% PR	846	771
9.6% PR	874	757

The level of restriction shown refers to measured energy intakes in the final week of study relative to 24 AL fed mice.
*Predictions for lifespans were evaluated based on the lifespan of 24AL control group which averaged 720 d.

value does not include the contribution of adipose tissue and organs' to work fueling. Maximum enthalpy efficiencies (i.e., first law efficiencies) for a variety of murine skeletal muscles were previously calculated as between 26% and 48% (27). These support the calculations performed here and are comparable to the first law efficiency of muscle work. Additionally, these values were close to experimental result of tortoise muscle energetic efficiency reported as 35% (28). The second law efficiencies were lower than the first law efficiencies (*SI Appendix*, Fig. S4 *A–D*) because the first law efficiency concept does not consider the best possible performance as a reference. However, in the second law efficiency assessments, the measure of actual performance is compared to the best possible performance under the same conditions. Second law efficiency evaluations can give an indication of system performance under reversible conditions. Correspondingly, if the second law efficiency is low, that means there is high irreversibility, and each irreversible process contributes to the entropy generation by the system. Therefore, an inverse relationship between second law efficiency and entropy generation rate would be expected. In the PR animals, where exergy content was very similar, this expected significant inverse relationship was found (R-square > 0.93, $P < 0.05$). However, in the CR groups fed variable exergy content, average daily entropy generation had a much stronger relationship with average daily exergy input (R-square > 0.99, $P < 0.05$), instead of with the average daily second law efficiencies. Because, with the decrement of exergy intake, total work outputs also decreased, and this caused the general decreasing trend in second law efficiencies, which is the ratio of these two variables. In our study, the inverse relationship between second law efficiency and entropy generation was observed when the exergy input was similar for the compared systems.

Implications of Entropy Generation Changes for Lifespan. The calculated lifespan increment percentages were compared with values from the literature, including the experimental lifespan increment percentages and the corresponding CR levels (18, 29) (Fig. 3*A*). Based on this comparison, the effect of CR level on lifespan was not as high as computationally predicted lifespans based

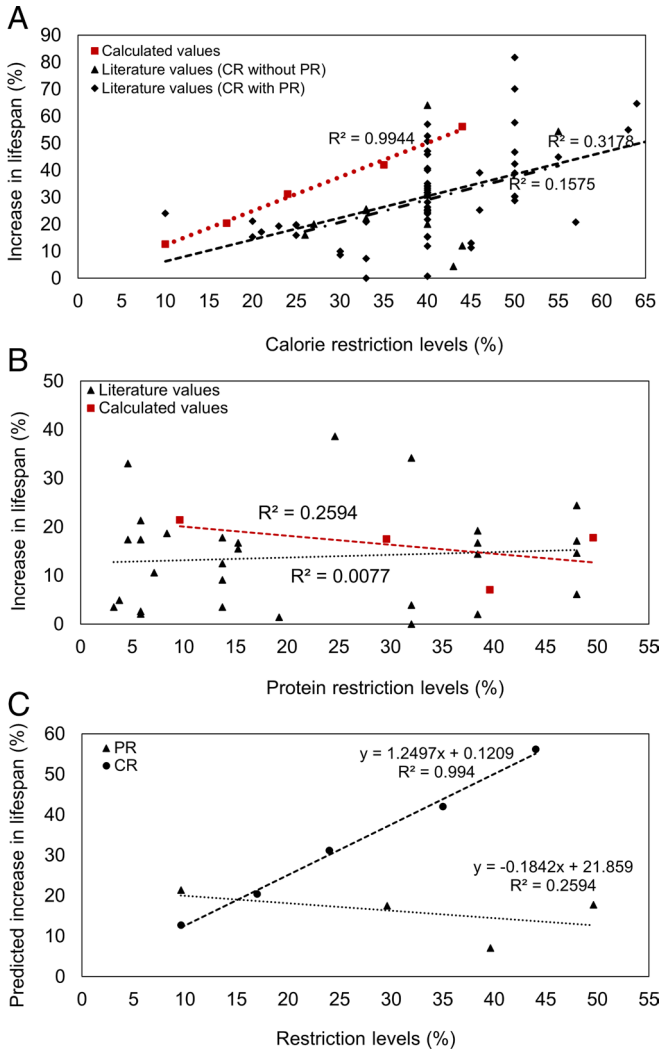

Fig. 3. Relationship between CR or PR and % increase in lifespan in mice (*A*) predicted lifespan modeled from 3 mo graded CR and PR data presented in current paper; (*B*) summarized CR data (18, 29); and (*C*) summarized PR data (18). The CR and PR data points are represented with ● and ▲ respectively, the line represents linear fitting. The level of restriction shown refers to measured energy intakes in the final week of study relative to 24 AL fed mice.

on the average daily entropy generation (Fig. 3*A*). There are several potential explanations for this discrepancy. In the current study, estimates of the entropy generation were based on the experimental data obtained over 3 mo, with the animals 8 mo old at the end of the study. In the lifespan calculation, we assumed that the calculated average daily entropy generation is maintained as same during the entire life of animals and the lifespan predictions were made based on this assumption. However, in reality, the average daily entropy generation may vary with time under restriction making the computational predictions more optimistic than the experimental lifespan results (Fig. 3*A*). The discrepancy would be consistent with entropy generation accelerating at later ages.

Dietary protein percent values in the study of Speakman et al. (18) were converted to PR percentages based on the baseline from our study, these were then compared with our computational results in Fig. 3*B*. It seems that PR level had a very heterogenic/random effect on the lifespan increment based on literature (18). While the calculated predicted lifespan increments for CR diets were higher, calculations for the PR diets were within the range of the literature values (Fig. 3 *A* and *B*). The regression equations

were extracted from studies to find the empirical relationship between the % increase in lifespan and CR and PR (18). In the current study, these equations are also evaluated to calculate lifespan day predictions, and these days are compared with the introduced thermodynamical modeling predictions (Table 1). Our model predicts a higher lifespan for all CR and PR groups bar the 39.6% PR (Table 1). The difference in calculated lifespan days was higher where the CR was higher; however, in the PR animals, the difference in lifespan days decreased with increasing restriction levels (Fig. 3 *A* and *B*).

Notably, the relationship between PR level and extension of lifespan was negative (Fig. 3*C*). The effect of PR on the lifespan of rodents has been previously reviewed in detail (18). Although diets with reduced protein content may increase the median lifespan (17, 30), the effect is only apparent with much lower levels of protein than tested here. This previous analysis emphasized that PR is effective but over a different range of restriction levels than CR works (18). This current computational research revealed a similar observation (Fig. 3*C*). With regard to the PR groups, although the protein amount was decreased, the same energy or exergy content was provided to all PR groups, therefore "predicted lifespan increment percentages" of these groups were also close to each other and had a significant linear relationship with exergy intake of PR groups (R-square > 0.94, $P < 0.05$) but had no significant relationship with the PR percentage levels ($P > 0.05$) (Fig. 3*C*). However, a strong linear relationship (R-square > 0.99, $P < 0.05$) between the predicted lifespan increment percentages and CR level was observed. This result parallels the suggestion that the effect of food restriction on lifespan is primarily due to reduced calories and not reduced protein intake (18). Refining the prediction using modeling of empirical data over a more extended period would be necessary to test this idea, but such data are currently not available.

The current data show that the impacts of CR and PR on the rate of entropy generation produced mean lifespan estimates that are broadly consistent with the actual impacts of these manipulations on published mean lifespan in rodents. Hence the data provide some support for the entropy generation model for lifespan and aging as originally proposed by Schrodinger in 1944 (1). This work therefore establishes as a concept the idea that quantifying entropy generation rates may provide a framework for evaluating diverse manipulations that potentially impact lifespan. Moreover, understanding the physiological processes that are connected to entropy changes will potentially provide a mechanism for identifying novel targets for aging interventions. Under fixed dietary conditions, individuals vary in how long they live and also in their individual entropy generation rates. A major goal for future work is to delineate whether these individual differences in entropy generation and lifespan are connected, or whether individual lifespan is dominated by unpredictable stochastic events. If individual lifespan is predictable from individual variation in entropy generation this would yield the potential to predict when an individual will die—a key goal in precision gerontology.

Conclusion

Life generates entropy (disorder), but the rate at which it does so is not the same across all conditions. Entropy probably accumulates because the cost to reverse its increase is too great. Schrodinger (1) suggested that ultimately we age and die because of this entropy accumulation. In other words, we die because the bodily system becomes so disordered that it can no longer sustain the functions we recognize as living. This idea has never been directly tested by quantifying the rate of entropy accumulation across different conditions and seeing if that matches the differences in observed lifespan. Here, we performed such entropy generation calculations for mice engaged in CR and PR and showed that the broad patterns of lifespan response to these manipulations can be predicted from entropy generation rates consistent with Schrodinger's hypothesis (1)

Materials and Methods

Data from male C57BL/6 mice undergoing 3 mo of graded CR or PR were adapted for thermodynamic assessment (22, 31–33). Control mice, fed ad libitum for 12 and 24 h are referred to as 12AL and 24AL groups, respectively. While designing the CR experiments, the average levels of restrictions were stated as 10, 20, 30, and 40% CR relative to their individual baseline 12AL intakes prior to the CR phase of the study. However, if the food intake of 12AL, 10, 20, 30, and 40% CR groups are compared relative to the average intake of the 24AL group in the final week, the approximate values of the percentage levels of restrictions become 9.6, 17, 24, 35, and 44%, respectively (31). In the PR study, the control group was fed 12AL with the same diet, 20% protein, as the CR study (31). Accordingly, restriction levels of the PR groups were calculated as 29.6, 39.6, and 49.6% relative to the 24AL group, respectively. PR diets were formulated by substituting the reduced protein with carbohydrates; the three PR diets were calorically equal (31). The following assumptions were considered while carrying out the analysis:

The resting metabolic rate (RMR) was assumed to be the same as the total internal work ($W_{int,total}$). Internal work performance, which was depicted as "internal work sink subsystem" in Fig.1, was fueled by both adipose tissue and the utilized organs, in addition to cellular metabolism.

Energy expense of organ investment ($W_{int,1}$) was part of the total internal work cost and fueled only with energy coming from the metabolism of nutrients.

On some occasions, a fraction of the energy provided by the food was accumulated in the adipose tissue ($E_{adipose}$). Otherwise, adipose tissue functioned as an internal energy source and provided energy to fuel a part of the internal work ($W_{int,2}$).

All the energy obtained from organ utilization fueled part of the internal work ($W_{int,4}$).

In the external (muscular) work (W_{ext}) calculations, work against friction is not accounted for.

The residual internal work energy expense was calculated after subtracting $W_{int,1}$, $W_{int,2}$ and $W_{int,4}$ from the total internal work ($W_{int,total}$). The residual internal work ($W_{int,3}$) energy expense was fueled with the energy coming from the cellular metabolism.

It was assumed that the energy utilized from the adipose tissue and organs entered the internal work sink subsystem and used only for work; however, the total internal heat output ($Q_{int,total}$) was fueled only by cellular metabolism.

According to the information provided by the supplier of the mice (Charles-River), the average 50% survival rate for male C57BL/6J mice fed a diet similar to that used in the CR study was around 720 d. In the current study, this lifespan was assumed to be the same for control (24AL) groups.

Energetic Assessments.

Daily invested or utilized organ energy assessment. Natural logarithm (LN) equations for body mass versus the mass of each organ at the final dissection of all individuals in the CR study were previously given (31). These LN equations and daily body mass data were used to calculate the daily masses of each organ of the CR groups.

For the PR groups, the total mass changes of each organ from the first to the final day of the experiment were divided into the number of days on study, and these mass change ratios of organs were assumed to be the same for each day.

To calculate the daily dry mass of the organs, the water content of each organ was employed (31). As previously suggested, the energy equivalent of the lean tissues was 17 kJ/g on dry basis (34). Based on daily mass and energy equivalent data, the total energy invested on organs ($W_{int,1}$) and the total energy extracted from the utilized organs ($W_{int,4}$) were calculated.

Daily invested or utilized adipose tissue energy assessment. The interpolated daily adipose tissue masses of the CR groups were estimated from the given LN fit equations of brown adipose tissue + epididymal + retroperitoneal + subcutaneous + mesenteric white adipose tissue mass versus body mass of the individuals in Mitchell et al. (31).

In PR groups, linear model equations (R-square > 0.70) were extracted from the pool of the dissected white and brown adipose tissue mass versus the total body mass data, and then these equations were used for interpolation, i.e., estimate the daily total adipose tissue mass.

The mean adipose tissue water content was 27% and a gram of dry adipose tissue provides 39.5 kJ of energy when utilized (31). Based on daily mass and energy equivalent data, daily energy investment to or energy obtained from the adipose tissue was calculated. Daily energy obtained from the adipose tissue ($W_{int,2}$) was assumed to be allocated to perform a fraction of the total internal work. It was also assumed that the energy expenditure of daily energy investment to adipose tissue ($E_{adipose}$) was only allocated from the extracted food energy via metabolism.

Daily energy loss as feces. In the study of Mitchell et al. (31) apparent energy assimilation efficiency (AEAE%) of both CR and PR groups was calculated at baseline and at the end of the study. In the current study, these AEAE% values and food intake (dry) of the CR and ad libitum individuals at baseline and at the end of the study were used to extract a linear model equation ($P < 0.05$, R-square > 0.24). In order to calculate the daily AEAE% values of each CR group, this linear model and the daily food intake (dry) of each CR group (31) were used. However, for PR groups there was no significant relationship between AEAE% and food intake (dry); therefore, average AEAE% values of PR individuals calculated at the end of the study were assumed as same for all days of the study (data adapted from ref. 31).

For both CR and PR groups, daily energy loss from feces (E_{DELF}) was calculated based on the daily energy uptake with consumed major food components ($\Delta h_{major\ food\ molecules}$) and daily AEAE%:

$$E_{DELF} = \left(\Delta h_{major\ food\ molecules}\right) \times (1 - AEAE\,\%) \qquad [2]$$

The value of $\Delta h_{major\ food\ molecules}$ refers to enthalpy (i.e., internal energy for this study) of chemical components in the diets and is calculated via Eq. **6** as explained at the related section in methodology.

Daily internal work performance. Adipose tissue serves mainly as an energy store and in contrast to muscle carries out no metabolic activity (13). Daily fat-free masses of groups were calculated by means of daily total body and daily adipose tissue masses that were calculated by LN fit equations in the adipose tissue energy assessment part. RMR (data adapted from ref. 33) and fat-free mass values of the CR individuals collected at the end of restriction were correlated ($P < 0.05$, R-square > 0.76). The daily RMR values of the CR groups were calculated with interpolation from this equation and the daily fat-free-mass data of CR groups. No relationship between the RMR and the fat-free-masses was found with the PR mice (R-square > 0.33); therefore, averages of the RMRs values from the end-of the-restriction period of each group were employed in those calculations (data adapted from ref. 33). In both CR and PR groups, the daily RMR values were considered to be equivalent to the total internal work $W_{int,\,total}$ [i.e., total of $W_{int,1}$ $W_{int,2}$ $W_{int,3}$ and $W_{int,4}$ (Fig. 1)].

Daily external work performance. Physical activity (counts per hr) measured (22) using the VitalView™ telemetry and data acquisition system (MiniMitter) and corresponding daily distance traveled (m) (Homecage Scan) (35) were used to generate a linear model equation ($P < 0.05$, R-square > 0.65). Using this equation, the daily distance traveled (m), Δ_x, of CR and PR animals was calculated and employed to calculate the external work (W_{ext}) by using general displacement work, W_x formula:

$$W_{ext} = W_x = F_x \times \Delta_x \qquad [3]$$

$$F_x = m \times g \qquad [4]$$

where F_x is the force; m is the body mass of a mouse and g is the gravitational acceleration.

Daily Δh_{rxn} of the oxidation reactions of foods. A full component list of the diet was obtained from the supplier (Research Diets). The standard enthalpy of formation ($\Delta h^\circ_{f,298.15K}$) of each major food component was obtained either from the literature (*SI Appendix*, Table S1) or calculated by the group contribution method as described by Eq. **5** (36):

$$\Delta h^\circ_{f,298.15K} = 68.29 + \sum_{i=1}^{n_{groups}} n_{i,group} \times \Delta h^\circ_{f,i,group} \qquad [5]$$

where, n_{groups} is the number of the atomic groups contained in the molecule; n_i is the number of the atomic groups i contained in the molecule and $\Delta h^\circ_{f,i,group}$ is the enthalpy of the atomic group i. All the values were corrected using Eq. **6** (36) for the daily changing average body temperature, T (22);

$$\Delta h_{f,T} = \left(\Delta T \times c_{p,298.15K}\right) + \Delta h^\circ_{f,298.15K} \qquad [6]$$

Some of the specific heat capacities, c_p, at standard temperature, 298.15 K, are available in the literature (*SI Appendix*, Table S1), the others were calculated by using modified Kopp's rule as previously described (37);

$$c_p = \sum_{i=1}^{N_i} n_E \times c_E \qquad [7]$$

where c_E is the specific heat constant of each element of the molecule at liquid and solid phases as listed (37).

The mole number of each component in the oxidation reactions were calculated from the stoichiometric balances given in *SI Appendix*, Table S1. They were multiplied with $\Delta h_{f,T}$ (kJ/mol) at the average daily body temperature. Energy extracted from the nutrients via cellular metabolism was calculated from Δh_{rxn} of the oxidation reactions of CR and PR groups as described (38).

Entering energies to cellular metabolism subsystems were calculated after subtracting the fecal energies from Δh of the major molecules of the food consumed.

$$\underbrace{\Delta h_{CO_2+H_2O+urea}}_{\sum \Delta h_{products}} - \underbrace{\left[\left(\Delta h_{major\ food\ molecules} - E_{faeces}\right) + \Delta h_{O2}\right]}_{\sum \Delta h_{reactants}} = \Delta h_{rxn} \qquad [8]$$

Energy balance around the cellular metabolism subsystem and the first law efficiency. The first law of thermodynamics is summarized with Eq. **9**;

$$\sum_{in}\left[\dot{N}\left(h + e_p + e_k\right)\right]_{in} - \sum_{out}\left[\dot{N}\left(h + e_p + e_k\right)\right]_{out} + \left(\dot{Q}_{in} - \dot{Q}_{out}\right) + \left(\dot{W}_{in} - \dot{W}_{out}\right) = \frac{d\left[N\left(u + e_p + e_k\right)\right]_{system}}{d_t} \qquad [9]$$

where the $\dot{N}$ is the molar flux, h is the specific enthalpy, e_p is the specific potential energy and e_k is the specific kinetic energy of a molecule, and $\dot{Q}$ and $\dot{W}$ are the heat and work flow through the system boundaries. The right-hand side of Eq. **9** represents energy accumulation within the system boundaries and was neglected for selected open (a control volume) cellular metabolism subsystem (39). Besides, e_p and e_k constituents and $\dot{Q}_{in}$ and $\dot{W}_{in}$ through the selected subsystem were also neglected. Therefore, energy extracted from the food was considered to be the same as Δh_{rxn} for this study.

Respiratory quotient (RQ) was assumed as cellular metabolism efficiency. The actual daily energy inputs to the cellular metabolism were obtained after multiplying ΔH_{rxn} with RQ to exclude the unused part of the nutrients from the calculations. The energy investment to the adipose tissue, $E_{adipose}$, was subtracted from the absolute value of ΔH_{rxn} that multiplied with RQ (*SI Appendix*, Fig. S1) to calculate the net residual energy, which fuels the total work, W_{out} ($W_{int,1}$, $W_{int,3}$ and W_{ext}), and the heat, Q_{out} (Q_{int} and Q_{ext}), flows fueled by the cellular metabolism subsystem. Ultimately, energy balance (Eq. **9**) for this study becomes;

$$\left(\Delta h_{rxn} \times RQ\right) - E_{adipose} = Q_{out} + W_{out} \qquad [10]$$

Each term of Eq. **10** was calculated for all the CR and PR groups, for each day of the experiment and used to calculate daily heat flow, Q_{out}, from the cellular metabolism subsystem through energy balance. The resulting daily Q_{out} values were portioned to daily internal ($Q_{int,\,total}$) and external (Q_{ext}) heat flows by using the corresponding work ratios; "$W_{int,total}/W_{out,total}$" and "$W_{ext}/W_{out,total}$".

The first law efficiency of cellular metabolism subsystem was defined as the percentage of the work components fueled only by cellular metabolism, to the net extracted energy at cellular metabolism for this study:

$$W_{out}\,\% = \frac{Average\left(W_{int,1} + W_{int,3} + W_{ext}\right)}{Average\left(\left(\Delta h_{rxn} \times RQ\right) - E_{adipose}\right)} \times 100 \qquad [11]$$

W_{out} % was calculated daily for each group of the CR and PR animals.

Exergetic Assessments.

Calculation of the Gibbs free energy of formation and chemical exergies of the molecules. Exergy is the maximum work obtainable from a substance when brought from the state of the environment to the dead state by means of a process interacting with the environment (40). In the present study, chemical exergy, ex°_{chem}, is regarded as the total exergy of a molecule and can be calculated by using molecule's Gibbs free energy of formation, $\Delta g^{\circ}_{f,298.15K}$ value. The Joback method, as summarized (36) was used to calculate $\Delta g^{\circ}_{f,298.15K}$ as;

$$\Delta g^{\circ}_{f,298.15K} = 53.88 + \sum_{i=1}^{n_{groups}} n_{i,group} \times \Delta g^{\circ}_{f,i,group} \qquad [12]$$

where n is the number of the atomic groups contained in the molecule, n_i is the number of the atomic groups i contained in the molecule and $\Delta h^{\circ}_{f,i,group}$ is the enthalpy of the atomic group and obtained from literature (36). When the ionic strength, pH, and dilution effects on Gibbs free energy are neglected, Δg°_{f} may be calculated at different temperature as;

$$\Delta g_{f,T} = \left(\frac{T}{T_0} \times \Delta g^{\circ}_{f,298.15K} \left[1 - \frac{T}{T_0} \right] \times \Delta h^{\circ}_{f,298.15K} \right) \qquad [13]$$

where T_0 is the standard temperature (298.15 K) and T is the daily changing body temperature of the animals.

The standard molar chemical exergy of component i, $ex^{\circ}_{chem,i}$, is defined (40) as the sum of the molar Gibbs free energy change of the compound in the standard state when synthesized from its constituent elements ($\Delta g^{\circ}_{f,i}$) and the stoichiometric sum of the standard chemical exergies of the k number of elements ($n_{k,elements} \times ex^{\circ}_{chem,k,element}$) in their stable states at temperature T_0 and pressure P_0:

$$ex^{\circ}_{chem,i} = \left(\Delta g^{\circ}_{f,i} \right) + \left(\sum_{k=1}^{n_{elements}} n_{k,element} \times ex^{\circ}_{chem,k,element} \right) \qquad [14]$$

After combining Eqs. **13** and **14**, chemical exergy of a molecule at a different temperature, such as at the physiological temperature, can be calculated with Eq. **15**;

$$ex_{chem,T} = \left(\frac{T}{T_0} \times \Delta g^{\circ}_{f,298.15K} + \left[1 - \frac{T}{T_0} \right] \times \Delta h^{\circ}_{f,298.15K} \right) + \left(\sum_{k=1}^{n_{elements}} n_{k,element} \times ex^{\circ}_{chem,k,element} \right) \qquad [15]$$

In the present study, chemical exergies of the elements are obtained from literature (41). Ultimately, chemical exergies of each components of CR and PR diets ($ex_{chem,T}$) were calculated for each day at average daily body temperature of groups and summed up to calculate daily chemical exergy intake with diets of groups (*SI Appendix*, Fig. S3).

Daily chemical exergy intake and oxidation products. The daily chemical exergy of the molecules of the food consumed was calculated by Eq. **15** at the daily body temperature (*SI Appendix*, Fig. S3) as explained in previous section The mole numbers of O_2, CO_2, H_2O and urea participating in these reactions were calculated for CR and PR groups from the stoichiometry of the oxidation reactions. Then, those mole numbers were used in the calculations of daily chemical exergies of these molecules changing with daily average body temperature of each group.

Daily chemical exergy lost with feces. Energetic proportion and daily exergy intake with diets were used to calculate the daily exergy of the feces:

$$\frac{\text{Total daily } \Delta h \text{ of the major metabolizable food molecules}}{\text{Daily energy loss with faeces}} \approx \frac{\text{Total daily exergy of major metabolizable food molecules}}{\text{Daily exergy loss with faeces}} \qquad [16]$$

Calculation of daily chemical exergy of the adipose tissue. Fatty acid composition of adipose tissue of 8 to 10-wk-old wild C57BL/6 male mice given in the study of Čanadi et al. (42) and fatty acid composition of standard diet used in the current study were proportioned, and these ratios were employed to calculate the approximate mole numbers of the fatty acids in the adipose tissue of CR and PR animals. These mole numbers were then used to calculate (Eq. **15**) daily adipose tissue chemical exergy investment and expense of the CR and PR mice at daily body temperatures.

Exergy balance around the cellular metabolism subsystem and second law efficiency. The exergy concept is often applied in engineering to compute the maximum available energy that can be obtained from a system to produce useful work (2). The computation of exergies of all system components (e.g., molar flux with chemical molecules and heat and work fluxes) enables an exergy balance to be estimated around each selected system and correspondingly find discarded waste energy (i.e., the energy that could not be transferred to work due to irreversibilities), which is called exergy destruction.

In the current study, exergy balance was established around the cellular metabolism subsystem to calculate the daily exergy destruction (Eq. **17**):

$$\sum_{in} \left[\dot{N}\, ex \right]_{in} - \sum_{out} \left[\dot{N}\, ex \right]_{out} - \sum_{i} \left[1 - \frac{T_s}{T_{b,i}} \right] \dot{Q}_i - \dot{W} - \dot{E}x_{dest} = \frac{d\left[N\, ex \right]_{system}}{dt} \qquad [17]$$

The first term in Eq. **17** refers to the exergy (ex) of the entering mole fluxes ($\dot{N}$) (food and oxygen). This daily exergy input to the cellular metabolism was corrected after multiplying with the RQ values as similar to energetic assessment part. The second term refers to the total exergy of the leaving mole fluxes (carbon dioxide, water vapor, urea, and feces) and the exergy expense for adipose tissue increment. The third term in Eq. **17** is the exergy of heat transfer ($\dot{Q}_i$), where the T_s is the surrounding temperature (298.15 K) and T_b is the boundary temperature, that equals daily body temperature in this study. The exergy of work flow, $\dot{W}$, equals to itself, in accordance with the meaning of the "exergy," e.g., useful work. The last term on the left side of the equation refers to the exergy destruction ($\dot{E}x_{dest}$), i.e., the lost exergy. The term at the right side of Eq. **17** refers to the exergy accumulation in system boundaries. Similarly, with the energy balance, it was assumed that there is no exergy accumulation for open (a control volume) cellular metabolism subsystem. The energy that cannot be utilized in useful work, Ex_{dest}, causes increasing disorder in the system. The calculated exergy destruction values can be used to calculate entropy generation as will be explained in the next section.

In the second law efficiency assessments, the measure of actual performance is compared to the best possible performance under the same conditions. In other words, the second law efficiency measures the system performance relative to its performance under reversible conditions (2). In the present study, the second law efficiency, η_{II}, of the cellular metabolism subsystem is defined as the ratio of work fueled only by cellular metabolism to the maximum theoretical useful exergy:

$$\eta_{II}(\%) = \left(\frac{\dot{W}_{int,1} + \dot{W}_{int,3} + \dot{W}_{ext}}{\sum \left(\dot{N}\, ex \right)_{in} - \sum \left(\dot{N}\, ex \right)_{out}} \right) \times 100 \qquad [18]$$

Daily entropy generation and approximate lifespan prediction. To understand the relationship between the restriction level and lifespan, entropy generation values, which can be found by using exergy destruction values, can be considered as a scale in computational predictions. Daily entropy generation of CR and PR groups were calculated by using the conversion equation which includes exergy destruction ($\dot{E}x_{dest}$) and the standard temperature (T_0);

$$\dot{E}x_{dest} = T_0 \dot{S}_{gen} \qquad [19]$$

In the current study, the highest daily average entropy generation was observed in the 24AL group, therefore, the approximate total lifespan entropy generation for 24AL group was estimated by multiplying the total lifespan (720 d) with the average daily entropy generation (0.1028 kJ/K). The approximate total lifespan entropy generation which may be reached by the 24AL C57BL/6 mice was estimated as 74.051 kJ/K with a similar calculation approach in previous studies (10, 43, 44). The approximate lifespans of CR and PR groups may be estimated by dividing that value to the average daily entropy generation values of each group.

In both CR and PR experiments, 12AL groups were fed with the same diet, which equals to 9.6% restriction compared to 24AL group's food intake in the final week of

restriction (31). For that reason, all of the calculated results of 9.6% restriction groups in CR and PR studies were expected to be close to each other. Although it was not significant, there was a difference in both of the experimental and computational results of these two groups which might be due to some biological variations.

The summary for energy and exergy assessments methodology is also given as flowchart at *SI Appendix*, Figs. S7 and S8.

Data, Materials, and Software Availability. All the data generated in this work are in the paper or have been previously published.

ACKNOWLEDGMENTS. This research was financially supported by The Scientific and Technological Research Council of Turkey (TUBITAK), Science Fellowships and Grant Programs, application number of 1059B141801348. The original experimental study was funded by Biotechnology and Biological Sciences Research Council (BBSRC) BB/G009953/1 and the China Partnering Award BB/J020028/1.

Author affiliations: [a]Department of Food Engineering, Faculty of Engineering, Yeditepe University, Istanbul 34755, Turkey; [b]Institute of Biological and Environmental Sciences, University of Aberdeen, Aberdeen AB24 2TZ, Scotland, UK; [c]Department of Physiology, Faculty of Medicine, Yeditepe University, Istanbul 34755, Turkey; [d]Shenzhen Key Laboratory of Metabolic Health, Center for Energy Metabolism and Reproduction, Shenzhen Institutes of Advanced Technology, Shenzhen 518055, China; and [e]Institute of Genetics and Developmental Biology, Chinese Academy of Sciences, Beijing 100101, China

1. E. Schrodinger, *What is Life–the Physical Aspect of the Living Cell with Mind and Matter and Autobiographical Sketches* (Cambridge University Press, Cambridge, UK, 1944), pp. 70–73.
2. Y. A. Çengel, M. A. Boles, M. Kanoğlu, *Thermodynamics: An Engineering Approach* (McGraw-hill, New York, 2011).
3. L. Hayflick, Biological aging is no longer an unsolved problem. *Ann. N. Y. Acad. Sci.* **1100**, 1–13 (2007).
4. L. Hayflick, Entropy explains aging, genetic determinism explains longevity, and undefined terminology explains misunderstanding both. *Plos Genetics.* **32**, 2351–2354 (2007).
5. C. Yildiz, V. A. Bilgin, B. Yılmaz, M. Özilgen, Organisms live at far-from-equilibrium with their surroundings while maintaining homeostasis, importing exergy and exporting entropy. *Int. J. Exergy.* **31**, 287–301 (2020).
6. C. Silva, K. Annamalai, Entropy generation and human aging: Lifespan entropy and effect of physical activity level. *Entropy* **10**, 100–123 (2008).
7. L. Demetrius, S. Legendre, P. Harremöes, Evolutionary entropy: A predictor of body size, metabolic rate and maximal lifespan. *Bull. Math. Biol.* **71**, 800–818 (2009).
8. I. Aoki, Entropy flow and entropy production in the human body in basal conditions. *J. Theor. Biol.* **141**, 11–21 (1989).
9. I. Aoki, Entropy production in human lifespan: A thermodynamical measure for aging. *Age* **17**, 29–31 (1994).
10. C. A. Silva, K. Annamalai, Entropy generation and human aging: Lifespan entropy and effect of diet composition and caloric restriction diets. *J. Thermodyn.* **2009**, 1–10 (2009).
11. A. S. Semercïöz, B. Yılmaz, M. Özilgen, Entropy generation behaviour of the lean and obese rats shows the effect of the diet on the wasted lifespan work. *Int. J. Exergy* **26**, 359–391 (2018).
12. R. Weindruch, R. L. Walford, S. Fligiel, D. Guthrie, The retardation of aging in mice by dietary restriction: Longevity, cancer, immunity and lifetime energy intake. *J. Nutr.* **116**, 641–654 (1986).
13. J. R. Speakman, S. E. Mitchell, Caloric restriction. *Mol. Aspects Med.* **32**, 159–221 (2011).
14. C. L. Green, D. W. Lamming, L. Fontana, Molecular mechanisms of dietary restriction promoting health and longevity. *Nat. Rev. Mol. Cell Biol.* **23**, 56–73 (2022).
15. J. R. Speakman, C. Hambly, Starving for life: What animal studies can and cannot tell us about the use of caloric restriction to prolong human lifespan. *J. Nutr.* **137**, 1078–1086 (2007).
16. M. D. Piper, L. Partridge, D. Raubenheimer, S. J. Simpson, Dietary restriction and aging: A unifying perspective. *Cell Metab.* **14**, 154–160 (2011).
17. S. M. Solon-Biet *et al.*, The ratio of macronutrients, not caloric intake, dictates cardiometabolic health, aging, and longevity in ad libitum-fed mice. *Cell Metab.* **19**, 418–430 (2014).
18. J. Speakman, S. Mitchell, M. Mazidi, Calories or protein? The effect of dietary restriction on lifespan in rodents is explained by calories alone. *Exp. Gerontol.* **86**, 28–38 (2016).
19. M. Eastwood, *Principles of Human Nutrition* (Blackwell Science, 2003), p. 459.
20. D. Derous *et al.*, The effects of graded levels of calorie restriction: VI. Impact of short-term graded calorie restriction on transcriptomic responses of the hypothalamic hunger and circadian signaling pathways. *Aging (Albany NY)* **8**, 642–663 (2016).
21. P. Dilsiz *et al.*, MCH neuron activity is sufficient for reward and reinforces feeding. *Neuroendocrinology* **110**, 258–270 (2020).
22. S. E. Mitchell *et al.*, The effects of graded levels of calorie restriction: V. Impact of short term calorie and protein restriction on physical activity in the C57BL/6 mouse. *Oncotarget* **7**, 19147–19170 (2016).
23. I. Aoki, Effects of exercise and chills on entropy production in human body. *J. Theor. Biol.* **145**, 421–428 (1990).
24. A. M. Rahman, A novel method for estimating the entropy generation rate in a human body. *Therm. Sci.* **11**, 75–92 (2007).
25. J. Çatak, B. Yılmaz, M. Ozilgen, Effect of aging on the second law efficiency, exergy destruction and entropy generation in the skeletal muscles during exercise. *Int. J. Biomed. Biol. Eng.* **11**, 27–32 (2017).
26. A. S. Semercïöz, B. Yılmaz, M. Özilgen, Thermodynamic assessment of allocation of energy and exergy of the nutrients for the life processes during pregnancy. *Br. J. Nutr.* **124**, 742–753 (2020).
27. C. Barclay, Energetics of contraction. *Compr. Physiol.* **5**, 961–995 (2015).
28. R. Woledge, The energetics of tortoise muscle. *J. Physiol.* **197**, 685–707 (1968).
29. W. R. Swindell, Dietary restriction in rats and mice: A meta-analysis and review of the evidence for genotype-dependent effects on lifespan. *Ageing Res. Rev.* **11**, 254–270 (2012).
30. J. R. Slonaker, The effect of different per cents of protein in the diet. *Am. J. Physiol.* **96**, 547–556 (1931).
31. S. E. Mitchell *et al.*, The effects of graded levels of calorie restriction: I. Impact of short term calorie and protein restriction on body composition in the C57BL/6 mouse. *Oncotarget* **6**, 15902–15930 (2015).
32. S. E. Mitchell *et al.*, The effects of graded levels of calorie restriction: III. Impact of short term calorie and protein restriction on mean daily body temperature and torpor use in the C57BL/6 mouse. *Oncotarget* **6**, 18314–18337 (2015).
33. S. E. Mitchell *et al.*, The effects of graded levels of calorie restriction: VIII. Impact of short term calorie and protein restriction on basal metabolic rate in the C57BL/6 mouse. *Oncotarget* **8**, 17453–17474 (2017).
34. K. D. Hall, P. N. Jordan, Modeling weight-loss maintenance to help prevent body weight regain. *Am. J. Clin. Nutr.* **88**, 1495–1503 (2008).
35. E. P. Udoh, *Impacts of Calorie Restriction on Behaviour and Post-restriction Hyperphagia* (University of Aberdeen, 2020).
36. D. W. Green, R. H. Perry, *Perry's Chemical Engineers' Handbook* (McGraw-Hill Education, 1997).
37. J. E. Hurst Jr., B. Keith Harrison, Estimation of liquid and solid heat capacities using a modified Kopp's rule. *Chem. Eng. Commun.* **112**, 21–30 (1992).
38. M. Carlos, Human body exergy metabolism. *Int. J. Thermodyn.* **16**, 73–80 (2013).
39. M. Özilgen, E. Sorgüven, *Biothermodynamics: Principles and Applications* (CRC Press, USA, 2016).
40. I. Dincer, M. A. Rosen, *Exergy: Energy, Environment and Sustainable Development* (Elsevier, USA, 2012).
41. J. Szargut, Chemical exergies of the elements. *Appl. Energy.* **32**, 269–286 (1989).
42. G. Čanadi Jurešić, K. Percan, D. Broznić, Effect of dietary fatty acid variation on mice adipose tissue lipid content and phospholipid composition. *Croatian J. Food Technol. Biotechnol. Nutr.* **11**, 128–137 (2016).
43. K. Annamalai, I. K. Puri, M. A. Jog, *Advanced Thermodynamics Engineering* (CRC Press, Boca Raton, FL, 2002).
44. L. Kuddusi, Thermodynamics and lifespan estimation. *Energy* **80**, 227–238 (2015).